Organometallics 1991, 10, 2626-2630

New Compounds of Zirconium(II) and Hafnium(II): Synthesis and X-ray Crystal Structures of Novel Dimers of Formula $M_2X_4(\eta^6\text{-}C_6H_5PMe_2)_2(PMe_2Ph)_2$

F. Albert Cotton,* Piotr A. Kibala, Maoyu Shang, and William A. Wojtczak

Laboratory for Molecular Structure and Bonding, Department of Chemistry, Texas A&M University, College Station, Texas 77843

Received January 28, 1991

The reduction of MX_4, where M = Hf; X = Br, and M = Zr; X = I, with Na/Hg amalgam, followed by addition of 2 equiv of PMe_2Ph, yields the arene complex $M_2X_4(\eta^6\text{-}C_6H_5PMe_2)_2(PMe_2Ph)_2$. An X-ray crystal structure determination indicated that the pyramidal $M_2X_2P_2$ units are centered over and bound to the phenyl substituent of the phosphine on the adjacent metal center. Crystallographic parameters are as follows. $Hf_2Br_4(\eta^6\text{-}C_6H_5PMe_2)_2(PMe_2Ph)_2$ (1): triclinic space group $P\bar{1}$; $a = 9.090$ (4), $b = 13.823$ (3), $c = 15.524$ (6) Å, $\alpha = 101.50$ (3)°, $\beta = 93.18$ (4)°, $\gamma = 97.24$ (4)°, $V = 1890$ (1) Å^3, and $d_{calc} = 2.160$ g/cm^3 for two crystallographically independent but essentially identical molecules in the unit cell. The structure was refined to $R = 0.0525$ and $R_w = 0.0584$ with a data/parameter ratio of 8.5. $Zr_2I_4(\eta^6\text{-}C_6H_5PMe_2)_2(PMe_2Ph)_2$ (2): monoclinic space group $P2_1/c$, $a = 13.527$ (4), $b = 12.599$ (2), $c = 13.574$ (3) Å, $\beta = 119.34$ (2)°, $V = 2017$ (2) Å^3, and $d_{calc} = 2.046$ g/cm^3 for $Z = 2$. The structure was refined to $R = 0.0606$ and $R_w = 0.0769$ with a data/parameter ratio of 8.2. Molecular orbital calculations on the model complex $ZrI_2(PH_3)_2(C_6H_6)$, at the Fenske–Hall level, were conducted to elucidate the bonding between the metal center and arene ring. The calculations indicate that the HOMO is composed of a d_{xy} δ-type orbital on the zirconium and a formerly $e_2\Pi^*$ orbital on the arene.

Introduction

The low-oxidation-state chemistry of hafnium and zirconium is an area that has experienced only minimal growth. The paucity of suitable starting materials and solvents, and the air and moisture sensitivity of their compounds, makes their preparation difficult. Although, the potential gain in a greater understanding of the chemistry of zirconium and hafnium in lower oxidation states may be enormous, particularly in the area of catalysis,[1] there are only a relatively small number of reports on molecular compounds containing hafnium and zirconium in oxidation state 3,[2] and even fewer for oxidation state 2[3] (excluding those that contain Cp^- or COT^{2-}).

There have been numerous accounts of transition-metal complexes containing bound arenes,[4] although such complexes with early transition metals are decidedly less common.[3,5,6] As part of our research interest into synthesizing and structurally characterizing low oxidation state group IV compounds we have uncovered two types of novel arene complexes. We have previously reported a hafnium(II) arene complex of formula $Hf_2I_4(PMe_3Ph)_4(\mu\text{-}\eta^{12}\text{-arene})$ (where arene = benzene or toluene).[3a] This compex has an intriguing structure, in which each pyramidal $HfI_2(PMe_2Ph)_2$ unit is centered above and bound to each face of the arene ring. We would now like to report a similar arene complex that has each pyramidal MX_2P_2 unit bound to a phenyl substituent of a phosphine, through all six carbon atoms.

It would seem that a strong affinity exists between the MX_2P_2 unit and arene rings, most probably as a consequence of a synergistic donor–acceptor type of bonding. The existence of this dimeric compound, in which the metal–metal distance is on the order of 5.4 Å, gives clear indication that the dinuclear nature is not chemically essential and $MX_2(PR_3)_2(\eta^6\text{-arene})$ species may be attainable.

Experimental Section

All manipulations were carried out under an argon atmosphere by using standard vacuum-line and Schlenk techniques. The solvents were freshly distilled under nitrogen from the appropriate drying reagent. ZrI_4 was obtained from Cerac, and $HfBr_4$ and PMe_2Ph were purchased from Strem. They were used as received.

Synthesis of $Hf_2Br_4(\eta^6\text{-}C_6H_5PMe_2)_2(PMe_2Ph)_2$ (1). $HfBr_4$ (0.2491 g, 0.5 mmol), PMe_2Ph (0.15 mL, 1.05 mmol), and 1.0 M Na/Hg (1.1 mL, 1.1 mmol) were stirred vigorously in 20 mL of toluene for 36 h. During the period of reaction the solution color turned brown and a green-brown precipitate collected on the bottom of the reaction vessel. The brown solution was filtered through Celite (2 cm) into a Schlenk tube. The solution was then layered with 30 mL of hexane. An attempt at dissolving the remaining precipitate in additional toluene proved unsuccessful. The chemical nature of the precipitate was not established. Crystallization occurred in 2 days with the appearance of small highly air sensitive brown plates; the isolated crystalline yield was ca. 52 mg (17%).

Synthesis of $Zr_2I_4(\eta^6\text{-}C_6H_5PMe_2)_2(PMe_2Ph)_2$ (2). This material was synthesized in much the same manner as 1. ZrI_4 (0.5988 g, 1.0 mmol), PMe_2Ph (0.29 mL, 2.04 mmol) and 1.0 M Na/Hg (2.1 mL, 2.1 mmol) were stirred vigorously in 20 mL of toluene for 24 h. The solution color was greenish-brown upon

---

* Author to whom correspondence should be addressed.

(1) Cardin, D. J.; Lappert, M. F.; Raston, C. L. *Chemistry of Organo-Zirconium-and-Hafnium Compounds*; Ellis Horwood Limited: West Sussex, England, 1986.

(2) See for example: (a) Wengrovius, J. H.; Schrock, R. R.; Day, C. S. *Inorg. Chem.* **1981**, *20*, 1844. (b) Cotton, F. A.; Kibala, P. A.; Wojtczak, W. A. *Inorg. Chim. Acta* **1990**, *177*, 1. (c) Girolami, G. S.; Wilson, S. R.; Morse, P. M. *Inorg. Chem.* **1990**, *29*, 3200. (d) Cotton, F. A.; Diebold, M. P.; Kibala, P. A. *Inorg. Chem.* **1988**, *27*, 799. (e) Cotton, F. A.; Kibala, P. A. *Inorg. Chem.* **1990**, *29*, 3192 and references therein.

(3) See for example: (a) Cotton, F. A.; Kibala, P. A.; Wojtczak, W. A. *J. Am. Chem. Soc. 113*, **1991**, 1462. (b) Calderazzo, F.; Pallavicini, P.; Pampaloni, G. *J. Chem. Soc. Dalton Trans.* **1990**, 1813. (c) Troyanov, S. I.; Ribakov, V. B. *Metalloorg. Khim.* **1989**, *2*, 1382 and references therein.

(4) See arenes: (a) Wilkinson, G., Stone, F. G. A., Abel, E. W., Eds. *Comprehensive Organometallic Chemistry*; Pergamon Press: New York, 1982; Vol. 3-8. (b) Collman, J. P.; Hegedus, L. S.; Norton, J. R.; Finke, R. G. *Principles and Applications of Organotransition Metal Chemistry*, 2nd ed.; University Science Books: Mill Valley, CA, 1987; pp 158-164.

(5) (a) Thewalt, U.; Österle, F. *J. Organomet. Chem.* **1979**, *172*, 317. (b) Thewalt, U.; Stollmaier, F. *J. Organomet. Chem.* **1982**, *228*, 149.

(6) (a) Cloke, F. G. N.; Cox, K. P.; Green, M. L. H.; Bashkin, J.; Prout, K. *J. Chem. Soc., Chem. Commun.* **1981**, 117. (b) Cloke, F. G. N.; Green, M. L. H. *J. Chem. Soc., Chem. Commun.* **1979**, 127. (c) Goldberg, S. Z.; Spivack, B.; Stanley, G.; Eisenberg, R.; Braitsch, D. M.; Miller, J. S.; Abkowitz M. J. *J. Am. Chem. Soc.* **1977**, *99*, 110. (d) Stollamaier, F.; Thewalt, U. *J. Organomet. Chem.* **1981**, *208*, 327.

0276-7333/91/2310-2626$02.50/0

Table I. Crystal Data for $Hf_2Br_4(\eta^6\text{-}C_6H_5PMe_2)(PMe_2Ph)_2$ (1) and $Zr_2I_4(\eta^6\text{-}C_6H_5PMe_2)(PMe_2Ph)_2$ (2)

	1	2
formula	$C_{32}H_{44}Br_4Hf_2P_4$	$C_{32}H_{44}I_4Zr_2P_4$
fw	1229.2	1242.7
space group	$P\bar{1}$	$P2_1/c$
systematic absences	none	$(0,k,0)$, $k = 2n + 1$ and $(h,0,l)$ $l = 2n + 1$
a, Å	9.090 (4)	13.527 (4)
b, Å	13.823 (3)	12.599 (2)
c, Å	15.524 (6)	13.574 (3)
α, deg	101.50 (3)	90.00
β, deg	93.18 (4)	119.34 (2)
γ, deg	97.24 (4)	90.00
V, Å^3	1890 (1)	2017 (2)
Z	2	2
d_{calc}, g/cm^3	2.160	2.046
cryst size, mm	0.10 × 0.05 × 0.12	0.30 × 0.30 × 0.10, 0.30 × 0.25 × 0.15^d
μ(Mo Kα), cm^{-1}	98.226	37.173
data collection instrument	CAD-4	CAD-4
radiation (monochromated in incident beam)	Mo Kα (λ = 0.71073 Å)	Mo Kα (λ = 0.71073 Å)
orientation rflns: no.; range (2θ), deg	25; $20 < 2\theta < 27$	25; $20 < 2\theta < 30$
temp, °C	−50	21
scan method	$\omega - 2\theta$	$\omega - 2\theta$
data collection range, 2θ, deg	$4 \le 2\theta \le 46$	$4 \le 2\theta \le 45$
no. of unique data,	5209	2289
total with $F_o^2 > 3\sigma(F_o^2)$	3020	1508
no. of params refined	354	185
transmission factors, max, min	0.999, 0.865	1.000, 0.861, 0.999, 0.859^d
R^a	0.0525	0.0606
$R_{w^2}{}^b$	0.0584	0.0769
quality-of-fit indicator^c	1.381	1.804
largest shift/esd, final cycle	0.02	0.01
largest peak, e/Å^3	2.114	0.971

[a] $R = \sum||F_o| - |F_c||/\sum|F_o|$. [b] $R_w = [\sum w(|F_o| - |F_c|)^2/\sum w|F_o|^2]^{1/2}$; $w = 1/\sigma^2(|F_o|)$. [c] Quality-of-fit $= [\sum w(|F_o| - |F_c|)^2/(N_{obs} - N_{parameters})]^{1/2}$. [d] Two crystals used.

Table II. Positional and Equivalent Isotropic Displacement Parameters and Their Estimated Standard Deviations for $Hf_2Br_4(\eta^6\text{-}C_6H_5PMe_2)_2(PMe_2Ph)_2$

atom	x	y	z	B_{eqv},^{a} Å^2
Hf(a)	0.3032 (1)	0.96867 (7)	0.85782 (6)	1.70 (2)
Br(1a)	0.5058 (2)	0.8733 (2)	0.7776 (1)	2.40 (5)
Br(2a)	0.0603 (2)	0.8394 (2)	0.8513 (1)	2.57 (5)
P(1a)	0.3677 (6)	0.8733 (4)	0.9907 (3)	1.6 (1)
P(2a)	0.2166 (6)	0.9481 (5)	0.6832 (4)	2.2 (1)
C(11a)	0.356 (3)	0.738 (1)	0.950 (2)	2.8 (5)
C(12a)	0.237 (2)	0.881 (2)	1.077 (1)	2.9 (5)
C(13a)	0.551 (2)	0.900 (1)	1.052 (1)	1.5 (4)
C(14a)	0.679 (2)	0.906 (1)	1.001 (1)	2.1 (5)
C(15a)	0.819 (2)	0.908 (1)	1.042 (1)	1.6 (4)
C(16a)	0.841 (2)	0.905 (1)	1.136 (1)	1.7 (4)
C(17a)	0.709 (2)	0.862 (2)	1.174 (1)	2.3 (5)
C(18a)	0.567 (2)	0.861 (1)	1.132 (1)	1.6 (4)
C(21a)	0.361 (3)	0.996 (2)	0.616 (1)	3.1 (6)
C(22a)	0.161 (3)	0.819 (2)	0.626 (1)	3.0 (5)
C(23a)	0.056 (3)	1.001 (2)	0.650 (2)	5.0 (7)*
C(24a)	0.073 (2)	1.093 (2)	0.618 (1)	2.4 (5)
C(25a)	−0.048 (3)	1.139 (2)	0.607 (2)	3.5 (6)
C(26a)	−0.190 (3)	1.106 (2)	0.627 (2)	3.4 (6)
C(27a)	−0.205 (2)	1.019 (2)	0.663 (2)	3.1 (6)
C(28a)	−0.083 (2)	0.968 (2)	0.678 (1)	2.7 (5)*
Hf(b)	0.3815 (1)	0.52427 (7)	0.34427 (6)	1.89 (2)
Br(1b)	0.1779 (2)	0.6014 (2)	0.4395 (1)	2.74 (5)
Br(2b)	0.5204 (3)	0.6655 (2)	0.2734 (2)	3.31 (6)
P(1b)	0.5794 (6)	0.6324 (4)	0.4794 (4)	1.7 (1)
P(2b)	0.1553 (6)	0.5303 (4)	0.2209 (4)	2.1 (1)
C(11b)	0.551 (2)	0.766 (1)	0.503 (1)	2.3 (5)
C(12b)	0.774 (2)	0.640 (2)	0.454 (1)	2.2 (5)
C(13b)	0.585 (2)	0.603 (1)	0.589 (1)	1.8 (4)
C(14b)	0.710 (2)	0.651 (2)	0.655 (1)	2.2 (5)
C(15b)	0.701 (2)	0.647 (1)	0.740 (1)	1.9 (4)*
C(16b)	0.571 (2)	0.596 (2)	0.771 (1)	2.3 (5)
C(17b)	0.434 (2)	0.586 (2)	0.713 (1)	2.4 (5)
C(18b)	0.443 (2)	0.587 (1)	0.628 (1)	1.9 (5)
C(21b)	−0.032 (2)	0.472 (2)	0.238 (1)	3.0 (5)
C(22b)	0.122 (3)	0.660 (2)	0.219 (2)	3.3 (5)*
C(23b)	0.176 (3)	0.477 (2)	0.106 (2)	3.4 (5)*
C(24b)	0.284 (3)	0.523 (2)	0.062 (1)	3.3 (6)
C(25b)	0.315 (2)	0.483 (2)	−0.024 (1)	2.6 (5)
C(26b)	0.240 (3)	0.391 (2)	−0.063 (2)	3.4 (6)
C(27b)	0.133 (2)	0.343 (2)	−0.023 (1)	2.7 (5)
C(28b)	0.099 (3)	0.385 (2)	0.063 (2)	3.0 (5)

* Atoms were refined isotropically. [a] The equivalent isotropic displacement parameter, B_{eqv}, is calculated as $1/3[a^2a^{*2}B_{11} + b^2b^{*2}B_{22} + c^2c^{*2}B_{33} + 2ab(\cos\gamma)a^*b^*B_{12} + 2ac(\cos\beta)a^*c^*B_{13} + 2bc(\cos\alpha)b^*c^*B_{23}]$.

filtering through Celite (2 cm). The solution upon being layered with 30 mL of hexane yielded olive green plates in 2 weeks time. The crystals were isolated by decantation, yield ca. 130 mg (21%).

The characterization of the $M_2X_4(\eta^6\text{-}C_6H_5PMe_2)_2(PMe_2Ph)_2$ complexes by chemical analysis and IR and NMR spectroscopy was precluded by their chemical and physical properties. The low oxidation state and coordinative unsaturation of the metal center made these complexes highly sensitive to oxidation and nucleophilic attack. The solubility of crystalline 1 and 2 in toluene and most other common arenes was exceedingly small, and decomposition occurred in many alternate solvents.

X-ray Crystallography. Crystal Structure of $Hf_2Br_4(\eta^6\text{-}C_6H_5PMe_2)_2(PMe_2Ph)_2$ (1). A small crystal of 1 was mounted on a capillary tip with a thin layer of epoxy cement covering the surface. Geometric and intensity data were taken by an Enraf-Nonius CAD-4 automated diffractometer equipped with graphite-monochromated Mo Kα (λ = 0.71073 Å) radiation by procedures described previously.[7] All data were collected at −50 °C. The unit cell was indexed on 25 strong reflections in the range $20° \le 2\theta \le 27°$. The crystal system was found to be triclinic. The lattice dimensions were verified by axial photography. Least-squares analysis was used to refine the cell parameters and orientation matrix.

The intensity data were collected by the $\omega - 2\theta$ scan technique in the range $4° \le 2\theta \le 46°$. During data collection 3 intensity standards were collected at 3-h intervals and 3 orientation reflections were collected following every 200 reflections. Upon completion of the data collection azimuthal scans (ψ scans) of 6 reflections having the Eulerian angle χ near 90° were recorded. The data were corrected for Lorentz and polarization factors, and a semiempirical absorption correction was applied.[8] A decay correction was not needed.

The structure was refined successfully in the triclinic space group $P\bar{1}$. The positions of the two hafnium atoms were determined by direct methods. A subsequent determination of the coordination sphere of the two crystallographically distinct but essentially identical hafnium molecules was routine. The non-hydrogen atoms were located with alternating sequences of least-squares refinement and difference Fourier maps. The final Fourier map showed a peak of 2.114 e/Å^3 within 1 Å of both P(2b) and C(23b). Table I summarizes the data pertaining to the crystallographic procedures and refinement of complexes 1 and 2. The atomic positional parameters of 1 are given in Table II.

Crystal Structure of $Zr_2I_4(\eta^6\text{-}C_6H_5PMe_2)_2(PMe_2Ph)_2$ (2). The general procedures were routine and similar to those just previously described.[7] A small crystal was glued to the inside of a thin-walled capillary with epoxy cement. The capillary was then mounted on the goniometer head of a CAD-4 diffractometer. The data were collected as previously described. A slow decay of the

---

(7) (a) Bino, A.; Cotton, F. A.; Fanwick, P. E. *Inorg. Chem.* **1979**, *18*, 3558. (b) Walker, N.; Stuart, D. *Acta Crystallogr., Sect. A.: Found. Crystallogr.* **1983**, *39*, 158.

(8) (a) North, A. C. T.; Phillips, D. C.; Mathews, F. S. *Acta Crystallogr., Sect. A.: Cryst. Phys. Diffr., Theor. Gen. Crystallogr.* **1968**, *A24*, 351. (b) The calculations were performed with the Enraf-Nonius structure determination package on the VAX 11/780 computer at the Department of Chemistry, Texas A&M University, College Station, TX 77843.

Table III. Positional and Equivalent Isotropic Displacement Parameters and Their Estimated Standard Deviations for $Zr_2I_4(\eta^6\text{-}C_6H_5PMe_2)_2(PMe_2Ph)_2$

atom	*x*	*y*	*z*	B_{eqv},[a] Å^2
Zr	0.7137 (1)	0.4215 (2)	0.1264 (1)	2.44 (4)
I(1)	0.6009 (1)	0.2222 (1)	0.1115 (1)	4.25 (4)
I(2)	0.8449 (1)	0.4948 (2)	0.3547 (1)	4.06 (4)
P(1)	0.8911 (4)	0.2752 (5)	0.2031 (4)	3.3 (1)
P(2)	0.5482 (4)	0.5141 (5)	0.1646 (4)	2.9 (1)
C(11)	1.034 (1)	0.321 (2)	0.245 (1)	2.7 (5)
C(12)	1.097 (1)	0.363 (2)	0.340 (2)	4.8 (7)
C(13)	1.209 (2)	0.399 (2)	0.376 (2)	7 (1)
C(14)	1.254 (2)	0.401 (3)	0.315 (2)	8 (1)
C(15)	1.197 (2)	0.364 (2)	0.219 (2)	8.7 (7)
C(16)	1.075 (2)	0.320 (2)	0.172 (2)	7.8 (8)
C(17)	0.913 (2)	0.207 (2)	0.331 (2)	6.4 (7)
C(18)	0.872 (2)	0.168 (2)	0.113 (2)	6.1 (8)
C(21)	0.403 (1)	0.516 (2)	0.061 (1)	2.3 (4)
C(22)	0.355 (1)	0.418 (2)	0.000 (1)	3.2 (5)
C(23)	0.236 (2)	0.406 (2)	−0.078 (2)	4.2 (6)
C(24)	0.160 (1)	0.494 (2)	−0.082 (2)	4.3 (6)
C(25)	0.208 (2)	0.574 (2)	0.010 (2)	3.9 (5)*
C(26)	0.326 (1)	0.586 (2)	0.074 (1)	3.1 (5)
C(27)	0.572 (1)	0.654 (2)	0.202 (2)	4.1 (6)
C(28)	0.542 (2)	0.451 (2)	0.285 (2)	4.4 (6)

*Atoms were refined isotropically. [a] The equivalent isotropic displacement parameter, B_{eqv}, is calculated as $1/3[a^2a^{*2}B_{11} + b^2b^{*2}B_{22} + c^2c^{*2}B_{33} + 2ab(\cos\gamma)a^*b^*B_{12} + 2ac(\cos\beta)a^*c^*B_{13} + 2bc(\cos\alpha)b^*c^*B_{23}]$.

Table IV. Selected Listing of Bond Distances (Å) and Angles (deg) for $Hf_2Br_4(\eta^6\text{-}C_6H_5PMe_2)_2(PMe_2Ph)_2$[a]

Bond Distances

Hf(a)–Br(1a)	2.625 (2)	Hf(b)–Br(1b)	2.630 (2)
Hf(a)–Br(2a)	2.645 (2)	Hf(b)–Br(2b)	2.647 (3)
Hf(a)–P(1a)	2.735 (6)	Hf(b)–P(1b)	2.745 (5)
Hf(a)–P(2a)	2.729 (6)	Hf(b)–P(2b)	2.752 (6)
Hf(a)–C(13a)′	2.28 (2)	Hf(b)–C(13b)′	2.26 (2)
Hf(a)–C(14a)′	2.50 (2)	Hf(b)–C(14b)′	2.46 (2)
Hf(a)–C(15a)′	2.48 (2)	Hf(b)–C(15b)′	2.47 (2)
Hf(a)–C(16a)′	2.30 (2)	Hf(b)–C(16b)′	2.29 (2)
Hf(a)–C(17a)′	2.50 (2)	Hf(b)–C(17b)′	2.49 (2)
Hf(a)–C(18a)′	2.47 (2)	Hf(b)–C(18b)′	2.43 (2)
P(1a)–C(11a)	1.85 (2)	P(1b)–C(11b)	1.86 (2)
P(1a)–C(12a)	1.84 (2)	P(1b)–C(12b)	1.83 (2)
P(1a)–C(13a)	1.84 (2)	P(1b)–C(13b)	1.82 (2)
P(2a)–C(21a)	1.86 (2)	P(2b)–C(21b)	1.84 (2)
P(2a)–C(22a)	1.82 (2)	P(2b)–C(22b)	1.86 (3)
P(2a)–C(23a)	1.80 (3)	P(2b)–C(23b)	1.83 (2)
C(13a)–C(14a)	1.45 (3)	C(13b)–C(14b)	1.48 (3)
C(13a)–C(18a)	1.45 (3)	C(13b)–C(18b)	1.47 (3)
C(14a)–C(15a)	1.39 (3)	C(14b)–C(15b)	1.33 (3)
C(15a)–C(16a)	1.47 (3)	C(15b)–C(16b)	1.46 (3)
C(16a)–C(17a)	1.47 (3)	C(16b)–C(17b)	1.47 (3)
C(17a)–C(18a)	1.41 (3)	C(17b)–C(18b)	1.33 (3)

Bond Angles

Br(1a)–Hf(a)–Br(2a)	107.99 (7)	Br(1b)–Hf(b)–Br(2b)	108.01 (9)
Br(1a)–Hf(a)–P(1a)	84.4 (1)	Br(1b)–Hf(b)–P(1b)	84.8 (1)
Br(1a)–Hf(a)–P(2a)	76.5 (1)	Br(1b)–Hf(b)–P(2b)	76.3 (1)
Br(2a)–Hf(a)–P(1a)	77.4 (1)	Br(2b)–Hf(b)–P(1b)	76.6 (1)
Br(2a)–Hf(a)–P(2a)	82.3 (1)	Br(2b)–Hf(b)–P(2b)	82.6 (1)
P(1a)–Hf(a)–P(2a)	146.2 (2)	P(1b)–Hf(b)–P(2b)	146.0 (2)
P(1a)–Hf(a)–C(13a)′	82.9 (5)	P(1b)–Hf(b)–C(13b)′	83.3 (5)
Hf(a)–P(1a)–C(11a)′	111.6 (8)	Hf(b)–P(1b)–C(11b)	110.8 (7)
Hf(a)–P(1a)–C(12a)′	115.3 (8)	Hf(b)–P(1b)–C(12b)	114.5 (6)
Hf(a)–P(1a)–C(13a)′	121.1 (7)	Hf(b)–P(1b)–C(13b)	121.6 (6)
C(11a)–P(1a)–C(12a)	102 (1)	C(11b)–P(1b)–C(12b)	102 (1)
C(11a)–P(1a)–C(13a)	100 (1)	C(11b)–P(1b)–C(13b)	102.3 (9)
C(12a)–P(1a)–C(13a)	103.8 (9)	C(12b)–P(1b)–C(13b)	103 (1)
Hf(a)–P(2a)–C(21a)	115.1 (7)	Hf(b)–P(2b)–C(22b)	112.3 (7)
Hf(a)–P(2a)–C(22a)	113.7 (8)	Hf(b)–P(2b)–C(21b)	116.8 (8)
Hf(a)–P(2a)–C(23a)	120.0 (9)	Hf(b)–P(2b)–C(23b)	117.9 (8)
C(21a)–P(2a)–C(22a)	104 (1)	C(22b)–P(2b)–C(21b)	101 (1)
C(21a)–P(2a)–C(23a)	102 (1)	C(22b)–P(2b)–C(23b)	104 (1)
C(22a)–P(2a)–C(23a)	99 (1)	C(21b)–P(2b)–C(23b)	103 (1)
Hf(a)–C(13a)′–P(1a)′	138 (1)	Hf(b)–C(13b)′–P(1b)′	140 (1)
P(1a)–C(13a)–C(14a)	117 (1)	P(1b)–C(13b)–C(14b)	120 (1)
P(1a)–C(13a)–C(18a)	117 (1)	P(1b)–C(13b)–C(18b)	118 (1)
C(14a)–C(13a)–C(18a)	118 (2)	C(14b)–C(13b)–C(18b)	113 (2)
C(13a)–C(14a)–C(15a)	118 (2)	C(13b)–C(14b)–C(15b)	121 (2)
C(14a)–C(15a)–C(16a)	122 (2)	C(14b)–C(15b)–C(16b)	122 (2)
C(15a)–C(16a)–C(17a)	115 (2)	C(15b)–C(16b)–C(17b)	113 (2)
C(16a)–C(17a)–C(18a)	119 (2)	C(16b)–C(17b)–C(18b)	120 (2)
C(13a)–C(18a)–C(17a)	120 (2)	C(13b)–C(18b)–C(17b)	123 (2)
P(2a)–C(23a)–C(24a)	121 (2)	P(2b)–C(23b)–C(24b)	119 (2)
P(2a)–C(23a)–C(28a)	119 (2)	P(2b)–C(23b)–C(28b)	122 (2)

[a] Numbers in parentheses are estimated standard deviations in the least significant digits.

intensity standards was observed. When the intensity standards reached 62% of their initial value the data collection was interrupted and ψ scans of 6 reflections were initiated. The data collection was then completed with another crystal of similar dimensions. The data were corrected for Lorentz and polarization factors; decay and semiempirical absorption corrections were also applied.[8] The data were then merged with the help of the SHELX-86 program,[9] giving an agreement factor for merging of $R = 0.0525$.

The structure was solved in the uniquely defined monoclinic space group $P2_1/c$. The initial coordinates of the zirconium atom were derived from a direct methods analysis. The subsequent positions of all non-hydrogen atoms were obtained from iterative applications of least-squares refinement and difference Fourier maps. The atomic positional parameters are given in Table III.

Computational Procedures

Molecular orbital calculations[10] on the model compound $ZrI_2(PH_3)_2(C_6H_6)$ were carried out by applying the Fenske–Hall approximation to the Hartree–Fock molecular orbital method.[11] Metal atom basis functions were taken from Richardson[12] and were expanded with 5s and 5p functions that have a zirconium exponent of 2.20.[13] Clementi ζ basis sets[14] were used for the main-group elements, phosphorus, iodine, carbon, and hydrogen. The hydrogen atom exponent was set at 1.20. The atomic coordinates used in the calculation were taken from the crystal structure data of 2 and idealized to conform with the C_{2v} symmetry of the model. The hydrogen atom coordinates were calculated to preserve the C_{2v} symmetry. The coordinate system for $ZrI_2(PH_3)_2(C_6H_6)$ was chosen so that the origin was placed at the center of the C_6H_6 ring. The ring lies in the *XY* plane of the molecular coordinate system, and the *Z* axis is located along the Zr–ring centroid vector; the *X* axis lies in the I–Zr–I plane, and the *Y* axis lies in the P–Zr–P plane. For each atom a local right-handed coordinate system was designated as follows; the *z* axis of the local system points toward the origin for the zirconium and the carbon atoms, and toward the zirconium for the phosphorus and iodine atoms. The *z* axis of each hydrogen atom points toward the atom to which it is bound. The *x* axes are parallel to the *XY* plane of the molecular coordinate system.

Results and Discussion

Their are two crystallographically independent dinuclear molecules of 1 in the unit cell, each residing on a crystallographic inversion center. The two molecules (a and b) are essentially identical in their dimensions. An ORTEP drawing of molecule b, showing a side view, is depicted in Figure 1. A selected listing of bond distances and angles for molecules a and b of 1 is given in Table IV. The Hf–Br and Hf–P bond lengths have the following ranges and average values: Hf–Br, 2.625–2.647, 2.635 [5] Å; Hf–P, 2.729–2.752, 2.740 [4] Å. The C–C bond lengths of the metal-bound phenyl group have a range and average value of 1.33–1.48 and 1.43 [2] Å, respectively. The Hf–C distances cover a wide range, 2.26–2.50, with an average value of 2.41 [3] Å. The variation of the Hf–C bond lengths is

---

(9) Sheldrick, G. M. *SHELX-86, Program for Crystal Structure Determination*; University of Cambridge: Cambridge, England, 1986.

(10) The calculations were performed on the Microvax II computer at the Laboratory for Molecular Structure and Bonding, Texas A&M University.

(11) Fenske, R. F.; Hall, M. B. *Inorg. Chem.* **1972**, *11*, 768.

(12) Richardson, J. W.; Blackman, M. J.; Ranochak, J. E. *J. Chem. Phys.* **1973**, *58*, 3010.

(13) Barber, M.; Connor, J. A.; Guest, M. F.; Hall, M. B.; Hiller, I. H.; Meredith, W. N. E. *J. Chem. Soc., Faraday Trans. 2*, **1972**, *54*, 219.

(14) *IBM J. Res. Dev.* **1965**, *9*, 2 ("Table of Atomic Functions", a supplement to a paper by Clementi, E.)

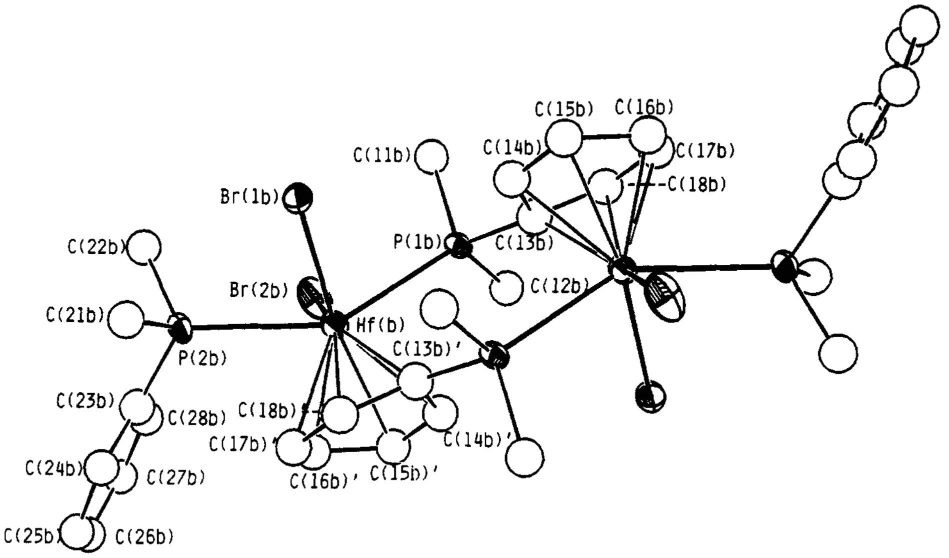

Figure 1. Side view of 1 (molecule b). Carbon atoms have been given arbitrary thermal parameters and heavy atoms are represented by their ellipsoids at the 50% probability level.

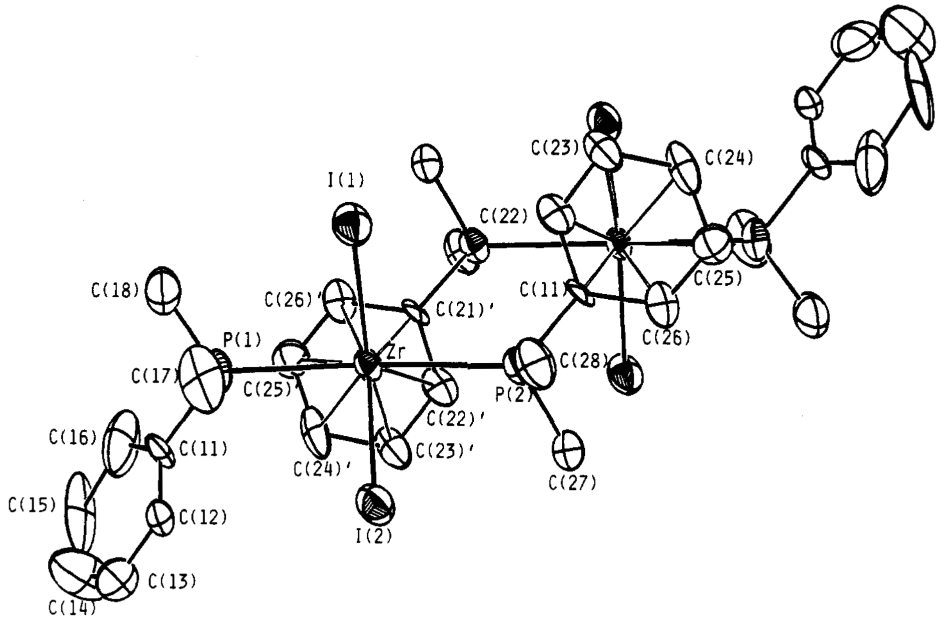

Figure 2. Top view of 2. Atoms are represented by their ellipsoids at the 50% probability level.

in accord with the ring puckering that is evident in Figure 1. Both carbon atoms 13 and 16 of molecules a and b lie an average 0.25 [1] Å closer to the hafnium as calculated from a least-squares plane drawn through carbon atoms 14, 15, 17, and 18. The nonplanarity of the ring and relatively long C–C bond lengths are suggestive of considerable donation of metal electron density into an empty component of the $e_2\Pi^*$ orbital of the ring.

Compound 2, which also resides on a crystallographic inversion center, is clearly structurally identical with 1. We have observed that depending on crystallization conditions 2 may either crystallize in the monoclinic space group $P2_1/c$ or in the triclinic space group $P\bar{1}$.[15] An ORTEP drawing of 2, viewed from above, is given in Figure 2. A listing of selected bond distances and angles is given in Table V. The average Zr–I and Zr–P bond lengths of 2.880 [4] and 2.790 [1] Å, respectively, are in good agreement with our previously reported average Hf–I and Hf–P bond lengths of 2.898 [4] and 2.787 [4] Å in the related complex $Hf_2I_4(PMe_2Ph)_4(\mu\text{-}\eta^{12}\text{-arene})$.[3a] This should be of no surprise since zirconium and hafnium in the same oxidation state and in similar chemical environment are of similar size, a consequence of the lanthanide contraction. The C–C and Zr–C bond lengths have ranges and average values of; 1.40–1.49, 1.46 [1] Å and 2.33–2.55, 2.46 [4] Å, respectively. There is, as in 1, a definite puckering of the bound ring, but a slightly more twisted conformation exists in 2. A least-squares plane drawn through carbon atoms 22, 23, 25, and 26 in 2 shows that these carbon atoms deviate to a greater extent from the plane than did those of 1. The C–C and Zr–C bond lengths of 2 can also be compared to those of $[(Me_6C_6)_3Zr_3Cl_6]^{2+}$,[6d] which possesses, as does 2, local (arene)ML_4 coordination geometry. The C–C and Zr–C bond lengths of $[(Me_6C_6)_3Zr_3Cl_6]^{2+}$ have ranges and average values of 1.39–1.48, 1.42 [4] Å and 2.55–2.63, 2.59 [3] Å, respectively. The shorter and longer average C–C and Zr–C bond lengths, respectively, in $[(Me_6C_6)_3Zr_3Cl_6]^{2+}$, as compared to 2, is most probably a consequence of the poorer overall donor–acceptor ability of the higher oxidation state zirconium centers.

---

[15] The cell parameters for crystallization in $P\bar{1}$ are similar to 1: $a = 9.211$ (1), $b = 14.449$ (2), $c = 16.045$ (2), $\alpha = 101.44$ (1)°, $\beta = 96.60$ (1)°, $\gamma = 96.68$ (1)°, $V = 2057.8$ (5) Å^3 at $T = 21$ °C.

Table V. Selected Listing of Bond Distances (Å) and Angles (deg) for $Zr_2I_4(\eta^6\text{-}C_6H_5PMe_2)_2(PMe_2Ph)_2$[a]

	Bond Distances		
Zr-I(1)	2.894 (3)	P(1)-C(17)	1.83 (3)
Zr-I(2)	2.866 (2)	P(1)-C(18)	1.76 (3)
Zr-P(1)	2.791 (6)	P(2)-C(21)	1.77 (1)
Zr-P(2)	2.789 (6)	P(2)-C(27)	1.82 (2)
Zr-C(21)′	2.37 (2)	P(2)-C(28)	1.85 (3)
Zr-C(22)′	2.52 (2)	C(21)-C(22)	1.45 (3)
Zr-C(23)′	2.46 (2)	C(21)-C(26)	1.46 (3)
Zr-C(24)′	2.33 (2)	C(22)-C(23)	1.44 (2)
Zr-C(25)′	2.55 (3)	C(23)-C(24)	1.49 (3)
Zr-C(26)′	2.51 (2)	C(24)-C(25)	1.49 (3)
P(1)-C(11)	1.82 (2)	C(25)-C(26)	1.40 (2)
	Bond Angles		
I(1)-Zr-I(2)	112.39 (8)	Zr-P(2)-C(28)	111.9 (8)
I(1)-Zr-P(1)	77.3 (1)	C(21)-P(2)-C(27)	100.9 (9)
I(1)-Zr-P(2)	86.1 (1)	C(21)-P(2)-C(28)	101.3 (9)
I(2)-Zr-P(1)	81.1 (1)	C(27)-P(2)-C(28)	104 (1)
I(2)-Zr-P(2)	78.0 (1)	P(1)-C(11)-C(12)	122 (2)
P(1)-Zr-P(2)	145.9 (2)	P(1)-C(11)-C(16)	121 (1)
P(2)-Zr-C(21)′	83.3 (5)	Zr-C(21)′-P(2)′	139 (1)
Zr-P(1)-C(11)	119.5 (7)	P(2)-C(21)-C(22)	118 (1)
Zr-P(1)-C(17)	111.7 (9)	P(2)-C(21)-C(26)	119 (1)
Zr-P(1)-C(18)	116.3 (7)	C(22)-C(21)-C(26)	116 (1)
C(11)-P(1)-C(17)	101.7 (9)	C(21)-C(22)-C(23)	122 (2)
C(11)-P(1)-C(18)	104 (1)	C(22)-C(23)-C(24)	117 (2)
C(17)-P(1)-C(18)	102 (1)	C(23)-C(24)-C(25)	118 (1)
Zr-P(2)-C(21)	122.1 (7)	C(24)-C(25)-C(26)	119 (2)
Zr-P(2)-C(27)	113.9 (8)	C(21)-C(26)-C(25)	122 (2)

[a] Numbers in parentheses are estimated standard deviations in the least significant digits.

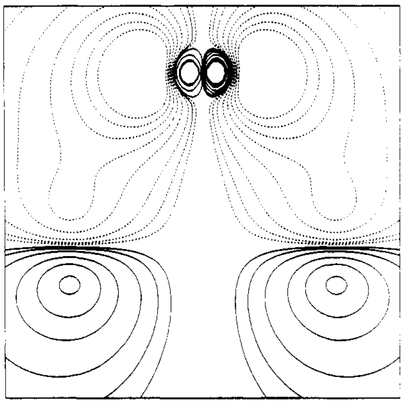

Figure 3. Contour plot of the HOMO of $ZrI_2(PH_3)_2(C_6H_6)$, in a plane lying 45° between the X and Y axes.

Having established some structural features of the $M_2X_4(\eta^6\text{-}C_6H_5PMe_2)_2(PMe_2Ph)_2$ complex we can now direct our attention to bonding considerations. We have employed the Fenske–Hall approximation to the Hartree–Fock method[11] to investigate the interaction between the MX_2P_2 pyramidal unit and the arene ring.[16] Our model compound, $ZrI_2(PH_3)_2(C_6H_6)$, has idealized C_{2v} symmetry. The calculations on the model compound result in a molecular orbital diagram with 32 doubly occupied valence molecular orbitals. We will concentrate the discussion on those orbitals that are responsible for bonding between the metal center and the arene. Our calculations indicate that the HOMO is formed by donation of metal d_{xy} electron density into an empty component of the arene $e_2\Pi^*$ orbital (the combined metal and carbon character is 82.2%). A contour plot in a plane perpendicular to the XY plane and lying 45° between the X and Y axes, is given in Figure 3. The plot depicts two of the carbon pΠ-orbitals interacting in a bonding fashion with two lobes of the metal d_{xy} orbital. Of the next six MO's lower in energy, two are I lone pair orbitals and four are Zr–I σ bonding orbitals. We then have the filled arene $e_1\Pi$ orbitals that donate moderately into the split (by 0.9 eV) metal d_{xz} and d_{yz} orbitals. The arene nondegenerate Π-orbital remains essentially unperturbed. The d_{z^2} orbital, with a small amount of mixed in $d_{x^2-y^2}$, interacts with the other component of the empty $e_2\Pi^*$ arene orbital to form the LUMO. A contour plot, in the XZ plane, is shown in Figure 4. A simplified MO diagram depicting the metal–arene orbital interactions is given in Figure 5.

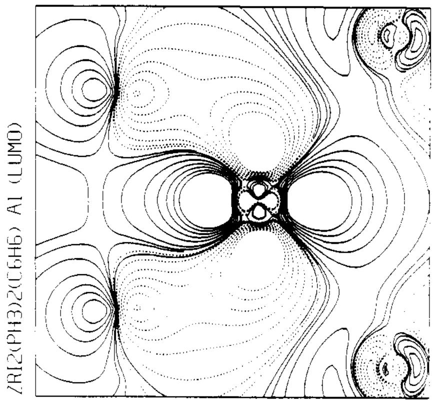

Figure 4. Contour plot of the LUMO of $ZrI_2(PH_3)_2(C_6H_6)$, in the XZ plane.

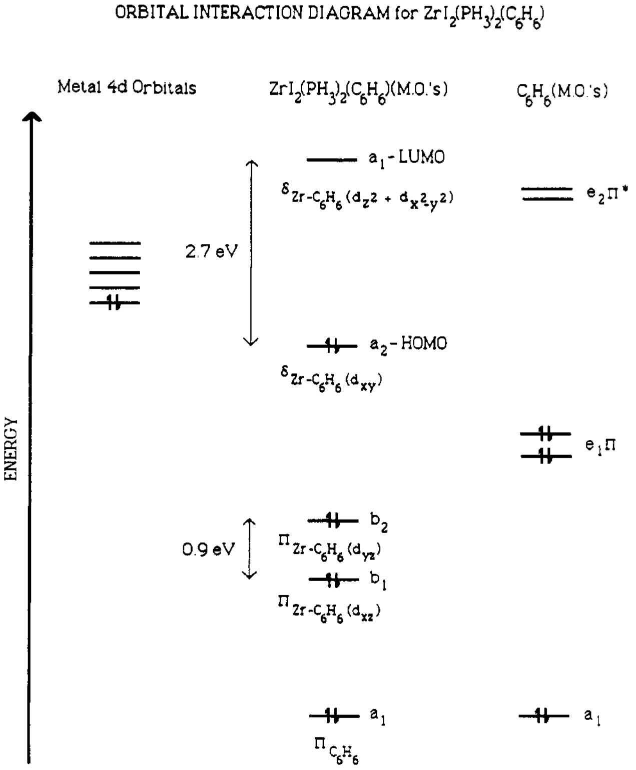

Figure 5. Metal–arene orbital interaction diagram for $ZrI_2(PH_3)_2(C_6H_6)$.

Acknowledgment. We thank the Robert A. Welch Foundation for support under Grant No. A 494.

Supplementary Material Available: Full listing of bond lengths and angles, thermal displacements, least-squares planes, unit cell diagrams, and valence molecular orbitals, their energies, and percent characters for $ZrI_2(PH_3)_2(C_6H_6)$ (36 pages); tables of observed and calculated structure factors (24 pages). Ordering information is given on any current masthead page.

---

(16) For additional information on metal-arene bonding see ref 4b and (a) Arney, D. J.; Wexler, P. A.; Wigley, D. E. *Organometallics* **1990**, *9*, 1282. (b) Anthony, M. T.; Green, M. L. H.; Young, D. *J. Chem. Soc., Dalton Trans.* **1975**, 1419.